

RARE B DECAYS AT BELLE

H.C. HUANG

(for the Belle Collaboration)

Department of Physics, National Taiwan University, Taipei 106, Taiwan



Recent results of rare B decay analyses based on 31.9 million $B\bar{B}$ collected with the Belle detector at the KEKB asymmetric e^+e^- collider are presented. We have made the first observation of charmless baryonic decay $B^\pm \rightarrow p\bar{p}K^\pm$, the three-body $B^0 \rightarrow K^0\pi^+\pi^-$ and $B^0 \rightarrow K^0K^+K^-$. The measured branching fractions are $\mathcal{B}(B^+ \rightarrow p\bar{p}K^+) = (4.3^{+1.1}_{-0.9} \pm 0.5) \times 10^{-6}$, $\mathcal{B}(B^0 \rightarrow K^0\pi^+\pi^-) = (53.2 \pm 11.3 \pm 9.7) \times 10^{-6}$, and $\mathcal{B}(B^0 \rightarrow K^0K^+K^-) = (34.8 \pm 6.7 \pm 6.5) \times 10^{-6}$. We also see strong evidence of $B^\pm \rightarrow \eta K^\pm$ and $B^\pm \rightarrow \eta\pi^\pm$, and observed the decay $B^\pm \rightarrow \omega K^\pm$ with $\mathcal{B}(B^\pm \rightarrow \omega K^\pm) = (9.9^{+2.7}_{-2.4} \pm 1.0) \times 10^{-6}$. Preliminary results of improved measurements of the branching fractions for the decays $B \rightarrow K\pi$ and $\pi\pi$ are reported. No evidence for direct CP violation is found in the decays $B^\pm \rightarrow K^\pm\pi^\mp$, $K^\pm\pi^0$, $K^0\pi^\pm$, $\pi^\pm\pi^0$, and ωK^\pm .

1 Introduction

One of the most important goals of experiments at B-factories is to precisely measure the sides and angles of the unitarity triangle in the Cabbibo-Kobayashi-Maskawa matrix³ (CKM) and check its consistency. Any inconsistency is a clear signal of new physics beyond the Standard Model (SM). Rare B decays play an important role in working towards this goal.

Preliminary results of rare B decay analyses based on a 31.9 million $B\bar{B}$ sample are presented here. The data were collected with the Belle detector¹ at the KEKB asymmetric e^+e^- collider.²

Belle is a general-purpose detector with a 1.5 T superconducting solenoid magnet. Charged particle tracking, covering 92% of the total center-of-mass (CM) solid angle, is provided by the Silicon Vertex Detector (SVD) consisting of three concentric layers of double-sided silicon strip detectors and a 50-layer Central Drift Chamber (CDC). Charged hadrons are distinguished by combining the responses from an array of Silica Aerogel Čerenkov Counters (ACC), a Time of Flight Counter system (TOF), and dE/dx measurements in the CDC. The combined response provides K/π separation of at least 2.5σ for laboratory momenta up to 3.5 GeV/ c . Photons and

Table 1: The signal yield, reconstruction efficiency (ϵ), statistical significance (Σ), branching fractions (\mathcal{B}), and the 90% confidence level upper limits (UL) for two-body B decay modes. All the results are preliminary.

Mode	Yield	ϵ	Σ	$\mathcal{B} (\times 10^{-6})$	UL ($\times 10^{-6}$)
$K^+\pi^-$	218 ± 18	0.31	16.4	$21.8 \pm 1.8 \pm 1.5$	-
$K^+\pi^0$	58 ± 11	0.15	6.3	$12.5 \pm 2.4 \pm 1.2$	-
$K^0\pi^+$	66 ± 10	0.32	8.2	$18.8 \pm 3.0 \pm 1.5$	-
$K^0\pi^0$	19 ± 8	0.23	2.7	$7.7 \pm 3.2 \pm 1.6$	-
$\pi^+\pi^-$	51 ± 11	0.31	5.4	$5.1 \pm 1.1 \pm 0.4$	-
$\pi^+\pi^0$	36 ± 11	0.16	3.5	$7.0 \pm 2.2 \pm 0.8$	-
$\pi^0\pi^0$	12 ± 6	0.13	2.2	-	< 5.6
K^+K^-	0 ± 2	0.26	0	-	< 0.5
K^+K^0	0 ± 2	0.17	0	-	< 3.8
K^0K^0	1 ± 3	0.20	0	-	< 13
ηK^+	-	-	4.9	$5.3^{+1.8}_{-1.5} \pm 0.6$	-
$\eta_{\gamma\gamma} K^+$	$12.7^{+5.0}_{-4.2}$	0.18	4.3	$5.7^{+2.2}_{-1.9}$	-
$\eta_{\pi^+\pi^-\pi^0} K^+$	$4.2^{+3.1}_{-2.3}$	0.15	2.4	$4.6^{+3.4}_{-2.5}$	-
$\eta\pi^+$	-	-	4.3	$5.4^{+2.0}_{-1.7} \pm 0.6$	-
$\eta_{\gamma\gamma}\pi^+$	$11.4^{+4.9}_{-4.1}$	0.16	3.8	$5.9^{+2.5}_{-2.1}$	-
$\eta_{\pi^+\pi^-\pi^0}\pi^+$	$4.0^{+3.1}_{-2.3}$	0.14	2.1	$4.8^{+3.7}_{-2.8}$	-
ωK^-	$19.7^{+5.4}_{-4.8}$	0.06	6.4	$9.9^{+2.7}_{-2.4} \pm 1.0$	-
$\omega\pi^-$	$10.6^{+4.8}_{-4.5}$	0.08	3.3	$4.3^{+2.0}_{-1.8} \pm 0.5$	< 8.2

electrons are detected in an array of 8736 CsI(Tl) crystals (ECL) located inside the magnetic field and covering the entire solid angle of the charged particle tracking system. The 1.5 T magnetic field is returned via an iron yoke, instrumented to detect muons and K_L mesons (KLM). The KLM consists of alternating layers of resistive plate chambers and 4.7 cm thick steel plates.

In all the decay modes presented here, the continuum process ($e^+e^- \rightarrow q\bar{q}$) is the dominant background. Since $B\bar{B}$ events are spherical while the continuum events are jet-like, we apply cuts on various event shape variables (such as sphericity, thrust angle, Fox-Wolfram moments, and the production angle of B) to suppress the background.

B candidates are identified using two kinematic variables: beam constrained mass: $M_{bc} = \sqrt{E_{beam}^2 - p_B^2}$, and the energy difference: $\Delta E = E_B - E_{beam}$. Here E_{beam} is the beam energy, p_B and E_B are the momentum and energy of a reconstructed B candidate, respectively, where all variables are defined in the $\Upsilon(4S)$ rest frame.

K/π separation is performed by applying a cut on the likelihood ratio, $L_K/(L_\pi + L_K)$, where L_K (L_π) is a kaon (pion) likelihood computed from information from the particle identification devices: specific ionization loss in the central drift chamber, photo-electron yield in the aerogel Cherenkov counters, and time-of-flight.¹

2 Two-Body Charmless Hadronic B Decays

These processes are manifestations of penguin or suppressed three amplitudes proportional to small couplings in hadronic flavor mixing (CKM matrix). Because of the absence of CKM favored $b \rightarrow c$ amplitudes, these decays are particularly sensitive to potentially new contributions from interference effects and virtual particles in loops.

2.1 $B \rightarrow \pi\pi, K\pi, KK$

The charmless hadronic B decays $B \rightarrow \pi\pi, K\pi$, and KK provide a rich sample to test the standard model and to probe new physics. Of particular interest are indirect and direct CP violation

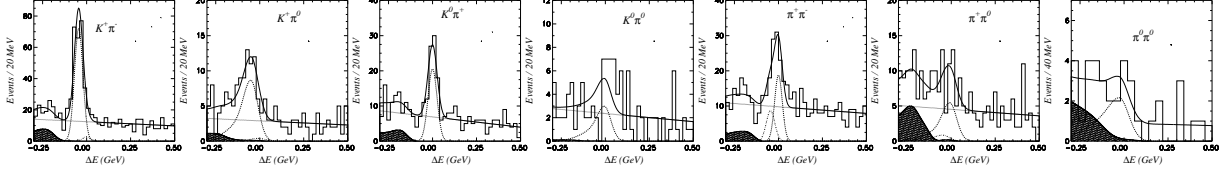


Figure 1: ΔE distributions of $B \rightarrow K\pi$ and $\pi\pi$ decays: (from left to right) $K^+\pi^-$, $K^+\pi^0$, $K_S^0\pi^+$, $K_S^0\pi^0$, $\pi^+\pi^-$, $\pi^+\pi^0$, and $\pi^0\pi^0$.

in the $\pi\pi$ and $K\pi$ modes, which are related to the angles ϕ_2 and ϕ_3 of the unitarity triangle, respectively.⁴ Measurements of branching fractions of these decay modes are an important step towards these CP violation studies.

In this analysis, B meson candidates are reconstructed in ten combinations: $h^+h'^-$, $h^+\pi^0$, $K_S^0h^+$, $K_S^0\pi^0$, $K_S^0K_S^0$, and $\pi^0\pi^0$, where the symbols h and h' refer to π or K . Candidate π^0 mesons are formed from pairs of photons and candidate K_S^0 mesons are reconstructed from pairs of oppositely charged tracks with a displaced vertex from the interaction point. Signal yields are extracted by fits to the ΔE distributions taking into account feed-across from other misidentified $B \rightarrow hh'$ decays and backgrounds from multi-body and radiative charmless B decays. The fit results are given in Table 1 and the ΔE distributions are shown in Figure 1.

2.2 $B^\pm \rightarrow \eta h^\pm$

Previous measurements^{5,6} yielded large rates for $B \rightarrow \eta' K$ and $B \rightarrow \eta K^*$, motivating a number of new theoretical ideas. Measurement of related decays $B \rightarrow \eta K$ can help clarify these. Besides, it has been suggested that the decays of $B^+ \rightarrow \eta\pi^+$ is a good candidate for observing direct CP violation.⁷

In this analysis, we reconstruct η mesons using the $\eta \rightarrow \gamma\gamma$ and $\eta \rightarrow \pi^+\pi^-\pi^0$ decay channels. Candidate η mesons are required to have invariant masses within $\pm 2.5\sigma$ of the η peak, where σ is $10.6 \text{ MeV}/c^2$ and $3.4 \text{ MeV}/c^2$ for the $\gamma\gamma$ and $\pi^+\pi^-\pi^0$ modes, respectively. For the $\pi^+\pi^-\pi^0$ mode, the $\pi^+\pi^-$ pair is constrained to a vertex. Both photons from the $\eta \rightarrow \gamma\gamma$ mode are required to have $E_\gamma > 100 \text{ MeV}$ and we remove η candidates if either of the daughter photons can be combined with any other photon with $E_\gamma > 100 \text{ MeV}$ to form a π^0 candidate. The η candidates are further constrained to the known η mass.⁸

Signal yields are obtained from extended unbinned maximum likelihood (ML) fits on the variables M_{bc} and ΔE . The signal probability density functions (PDF) are Gaussian for M_{bc} and an empirically determined parameterization⁹ for ΔE . The background PDF are taken to be an empirical function¹⁰ for M_{bc} and a first-order polynomial for ΔE . The statistical significance is defined as $\sqrt{-2\ln(\mathcal{L}(0)/\mathcal{L}_{\max})}$ where \mathcal{L}_{\max} is the likelihood at the nominal signal yield and

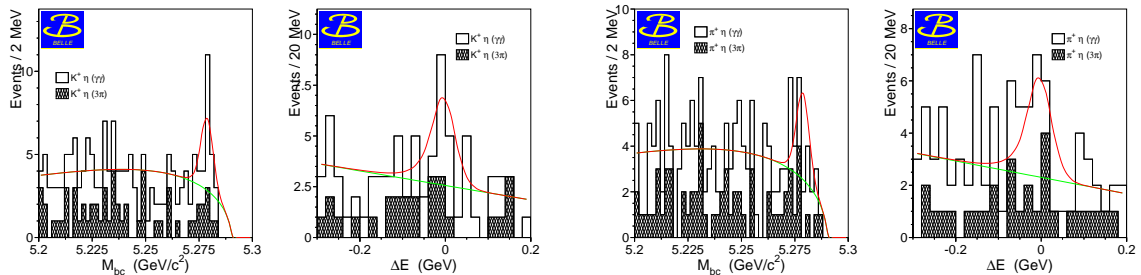


Figure 2: M_{bc} and ΔE distributions for (left) $B^\pm \rightarrow \eta K^\pm$ and (right) $B^\pm \rightarrow \eta\pi^\pm$. Histograms represent data, with the $\eta_{\pi^+\pi^-\pi^0}$ subset shaded, the solid curves represent the fit functions.

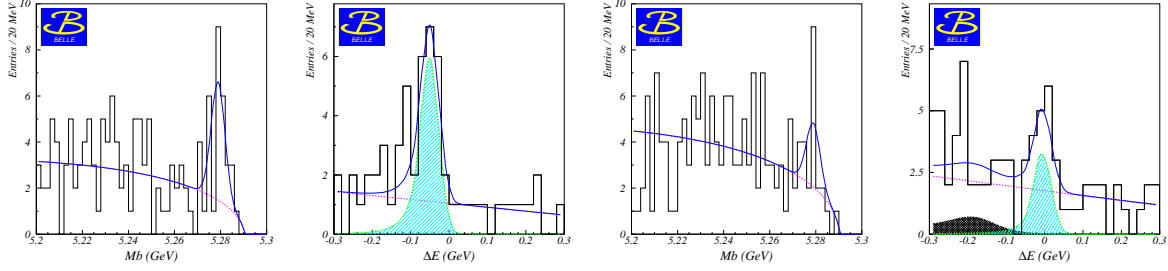


Figure 3: The M_{bc} and ΔE projections with the normalized signal and background PDFs for (left) $B^\pm \rightarrow \omega K^\pm$ and (right) $B^\pm \rightarrow \omega \pi^\pm$.

$\mathcal{L}(0)$ is the likelihood with the signal yield fixed to zero. The results of the fits for yields are given in Table 1. Figure 2 shows distributions of M_{bc} and ΔE with the projections of the fit function. We see strong evidence for the decays $B^\pm \rightarrow \eta K^\pm$ and $B^\pm \rightarrow \eta \pi^\pm$ with statistical significance of 4.9σ and 4.3σ , respectively. Assuming the number of $B^0\bar{B}^0$ and B^+B^- pairs to be equal, we find their branching fractions $\mathcal{B}(B^\pm \rightarrow \eta K^\pm) = (5.3^{+1.8}_{-1.5} \pm 0.6) \times 10^{-6}$ and $\mathcal{B}(B^\pm \rightarrow \eta \pi^\pm) = (5.4^{+2.0}_{-1.7} \pm 0.6) \times 10^{-6}$.

2.3 $B^\pm \rightarrow \omega h^\pm$

In this analysis, candidate ω mesons are reconstructed from $\pi^+\pi^-\pi^0$ combinations where the CM momentum of the π^0 is required to be greater than 350 MeV/c to reduce the large combinatorial background from low energy photons. The invariant mass of the $\pi^+\pi^-\pi^0$ combination is required to be within ± 30 MeV/ c^2 of the nominal ω mass⁸ (the natural width of the ω is 8.9 MeV/ c^2).

Signal yields are extracted using unbinned ML fit simultaneously for M_{bc} and ΔE . The background functions include a combinatorial component and a component from other charmless B decays. Due to the possible mis-identification between K^- and π^- , we also include a component for feed-down from $\omega\pi^-$ to ωK^- fitting and vice versa. If a pion is mis-identified to a kaon, the wrong mass assignment shifts the $\omega\pi^-$ signal 44 MeV away from zero, and the feed-down component from $\omega\pi^-$ can be distinguished in the ΔE distribution. The results of the fit are summarized in the Table 1. The projections of the M_{bc} and ΔE with the normalized signal and background PDFs are shown in Figure 3. We have observed the decay $B^\pm \rightarrow \omega K^\pm$ with 6.4σ significance. Our results on the $B^- \rightarrow \omega K^-$ and $\omega\pi^-$ branching fraction measurements disagree with the earlier ones from CLEO¹¹ and BABAR⁶. But the sum of the branching fractions of $B^- \rightarrow (\omega K^- + \omega\pi^-)$ is consistent with the CLEO's result.

3 Three-Body Charmless Hadronic B Decays

Belle has recently published results on tree body charmless hadronic decays $B^\pm \rightarrow K^\pm h^+ h^-$ ¹². It is of interest to look for similar phenomena in the neutral channel, to further investigate the $b \rightarrow s$ penguin transitions which mediate these decays. In addition, these modes may in future be used to measure CP violation.

3.1 $B^0 \rightarrow K^0 h^+ h^-$

In this analysis, we reconstruct the decays $B^0 \rightarrow K^0 h^+ h^-$ without any assumption on the intermediate hadronic resonance. Only $K^0 \rightarrow K_S^0 \rightarrow \pi^+\pi^-$ is considered here. As in other rare B decay modes, continuum events are the dominant background source and are suppressed using various event shape and kinematic variables. In the $B^0 \rightarrow K^0 \pi^+\pi^-$ mode, we also have large backgrounds from $B^0 \rightarrow D^-\pi^+$, $D^-\pi^+ \rightarrow K_S^0\pi^-$ and $B^0 \rightarrow J/\psi K_S^0$, $J/\psi \rightarrow \mu^+\mu^-$ where muons are

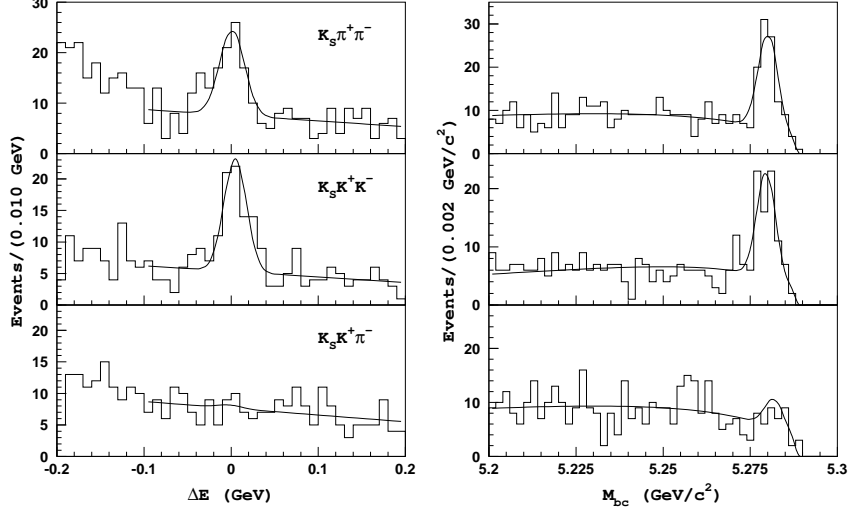


Figure 4: The ΔE (left) and M_{bc} (right) distributions for three-body final states: $K_S^0 \pi^+ \pi^-$ (top), $K_S^0 K^+ K^-$ (middle) and $K_S^0 K^+ \pi^-$ (bottom).

misidentified as pions. These backgrounds are suppressed by requiring $|M(K_S \pi^-) - M_{D^-}| > 0.100 \text{ GeV}/c^2$, $|M(h^+ h^-) - M_{J/\psi}| > 0.070 \text{ GeV}/c^2$, and $|M(h^+ h^-) - M_{\psi(2S)}| > 0.050 \text{ GeV}/c^2$, where h^+ and h^- are pion candidates. Signal yields are obtained from fits to the ΔE distributions. We find 60.3 ± 11.0 $B^0 \rightarrow K^0 \pi^+ \pi^-$ events and 57.9 ± 10.0 $B^0 \rightarrow K^0 K^+ K^-$ events, which corresponds to preliminary branching fractions:

$$\begin{aligned} \mathcal{B}(B^0 \rightarrow K^0 \pi^+ \pi^-) &= (53.2 \pm 11.3 \pm 9.7) \times 10^{-6}, \quad (6.6\sigma) \\ \mathcal{B}(B^0 \rightarrow K^0 K^+ K^-) &= (34.8 \pm 6.7 \pm 6.5) \times 10^{-6} \quad (7.4\sigma) \end{aligned}$$

Figure 4 shows the ΔE and M_{bc} distributions for these decays after the background suppression. We also search for $B^0 \rightarrow K^0 K^\pm \pi^\mp$ but do not observe significant signals. The 90% C.L. branching fraction upper limit is calculated to be $\mathcal{B}(B^0 \rightarrow K^0 K^\pm \pi^\mp) < 9.3 \times 10^{-6}$.

Further studies of intermediate resonant states of these decays are made with a Dalitz plot style analysis. Figure 5 shows the $\pi^+ \pi^-$ and $K_S^0 \pi^\pm$ invariant mass distributions for selected $B^0 \rightarrow K_S^0 \pi^+ \pi^-$ candidates in the B signal region, and the $K^+ K^-$ and $K_S^0 K^\pm$ invariant mass for $B^0 \rightarrow K_S^0 K^+ K^-$. Clear contributions from $K^*(892)^\pm \pi^\mp$ and $\phi(1020) K^0$ are seen. We also find broad resonances in $K_S^0 \pi^\pm$ and $K^+ K^-$ mass around $1.4 \text{ GeV}/c^2$ and $1.5 \text{ GeV}/c^2$, respectively. Assuming a set of two-body final states, we perform a simultaneous likelihood fit to the ΔE distributions for various resonance regions and determine the exclusive branching fractions. The uncertainty due to possible interference between different intermediate states is included as a model-dependent error. The results are summarized in Table 2.

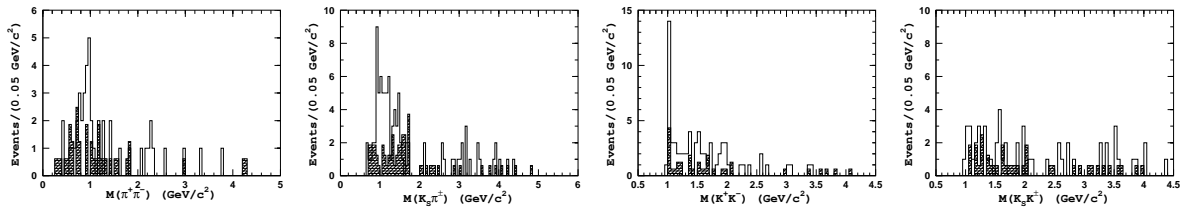


Figure 5: (a) $\pi^+ \pi^-$ and (b) $\pi^+ K_S^0$ invariant mass spectra for selected $B^0 \rightarrow K_S^0 \pi^+ \pi^-$, (c) $K^+ K^-$ and (d) $K^+ K_S^0$ for $B^0 \rightarrow K_S^0 K^+ K^-$, signal events (open histograms) and for background events in the ΔE sidebands (hatched).

Table 2: Preliminary results of the simultaneous fits to the $B^0 \rightarrow K^0 \pi^+ \pi^-$ and $K^0 K^+ K^-$ final states, respectively. Branching fractions of the corresponding decay modes from $B^+ \rightarrow K^+ h^+ h^-$ are also listed for comparison.¹²

Mode	ϵ (%)	Yield	Σ	$\mathcal{B}(B^0 \rightarrow Rh) \times \mathcal{B}(R \rightarrow hh) (\times 10^{-6})$	$\mathcal{B}(B^+ \rightarrow Rh^+) \times \mathcal{B}(R \rightarrow h^+ h^-)^{12} (\times 10^{-6})$
$K^*(892)^\pm \pi^\mp$	4.87 ± 0.23	$16.9^{+6.0}_{-5.2}$	3.9	$13.5^{+5.0}_{-4.4} \pm 2.9$	$12.9^{+2.8+1.4+2.3}_{-2.6-1.4-4.5}$
$K_X(1400)^\pm \pi^\mp$	4.22 ± 0.21	$24.9^{+9.0}_{-8.3}$	3.3	$22.9^{+8.7}_{-8.0} \pm 6.0$	$14.5^{+3.5+1.8+3.3}_{-3.3-1.8-6.5}$
$\rho^0(770)K^0$	4.56 ± 0.23	$1.4^{+6.4}_{-5.7}$	0.2	< 12.4	< 12 (90%CL)
$f_0(980)K^0$	5.22 ± 0.24	$9.4^{+6.0}_{-4.9}$	2.1	< 14.2	$9.6^{+2.5+1.5+3.4}_{-2.3-1.5-0.8}$
$f_X(1300)K^0$	5.27 ± 0.24	$8.0^{+6.0}_{-5.0}$	1.7	< 13.7	$11.1^{+3.4+1.4+7.2}_{-3.1-1.4-2.9}$
$\phi(1020)K^0$	7.01 ± 0.19	$11.7^{+5.5}_{-4.6}$	3.0	$6.4^{+3.0}_{-2.6} \pm 1.3$	$7.2^{+1.5+0.9+0.4}_{-1.4-0.9-0.4}$
$f_X(1500)K^0$	6.25 ± 0.18	$33.5^{+8.1}_{-7.5}$	5.3	$20.4^{+5.3}_{-4.9} \pm 3.8$	$27.6^{+3.2+3.5+1.4}_{-3.2-3.5-1.4}$
$a_0(980)^\pm K^\mp$	2.70 ± 0.38	$3.4^{+3.0}_{-2.4}$	1.5	< 12.1	—
$a_X(1300)^\pm K^\mp$	4.45 ± 0.09	$4.0^{+4.7}_{-4.1}$	1.0	< 10.0	—

4 Charmless Baryonic B Decays

In contrast to charm meson decay, final states with baryons are allowed in B meson decay. To date, a few low multiplicity B decay modes with baryons in the final state from $b \rightarrow c$ transitions have been observed.¹³ Rare B decays due to charmless $b \rightarrow s$ and $b \rightarrow u$ transitions should also lead to final states with baryons. A number of searches for such modes have been carried out by CLEO,¹⁴ ARGUS,¹⁵ and LEP¹⁶ but only upper limits were obtained. Stringent upper limits for two-body modes such as $B \rightarrow p\bar{p}$, $\bar{\Lambda}p$, and $\Lambda\bar{\Lambda}$ have recently been reported by Belle.¹⁷

4.1 $B^\pm \rightarrow p\bar{p}K^\pm$ ¹⁸

We have searched for the decay modes $B^\pm \rightarrow p\bar{p}K^\pm$ and $B^0 \rightarrow p\bar{p}K_S^0$. These modes are expected to proceed mainly via $b \rightarrow s$ penguin diagrams. We also search for $B^+ \rightarrow p\bar{p}\pi^+$ which is expected to occur primarily via a $b \rightarrow u$ tree process. Once they are established, these baryonic modes may be used to either constrain or observe direct CP violation in B decay.¹⁹

To reconstruct signal candidates in the $B^+ \rightarrow p\bar{p}K^+$ mode, we form combinations of a kaon, proton and anti-proton that are inconsistent with the following $b \rightarrow c\bar{c}s$ transitions: $B^+ \rightarrow J/\psi K^+$, $J/\psi \rightarrow p\bar{p}$; $B^+ \rightarrow \eta_c K^+$, $\eta_c \rightarrow p\bar{p}$; $B^+ \rightarrow \psi' K^+$, $\psi' \rightarrow p\bar{p}$ and $B^+ \rightarrow \chi_{c[0,1]} K^+$, $\chi_{c[0,1]} \rightarrow p\bar{p}$. This set of requirements is referred to as the charm veto. Similar charm vetoes are applied in the analysis of the other decay modes. In the case of $B^0 \rightarrow p\bar{p}K_S$, events with pK_S or $\bar{p}K_S$ masses consistent with the Λ_c are rejected.

In Figure 6, we show the ΔE distribution (with $5.27 \text{ GeV}/c^2 < M_{bc} < 5.29 \text{ GeV}/c^2$) and M_{bc} distribution (with $|\Delta E| < 50 \text{ MeV}$) for the signal candidates. We fit the ΔE distribution with a double Gaussian for signal and a linear background function with slope determined from the M_{bc} sideband. The fit to the ΔE distribution gives a yield of $42.8^{+10.8}_{-9.6}$ with a significance of 5.6σ . This is the first observation of a $b \rightarrow s$ transition with baryons in the final state.

We also examine the $M_{p\bar{p}}$ mass distributions for events in the ΔE , M_{bc} signal region. The signal yield as a function of $p\bar{p}$ mass is shown in Figure 6(c). These yields were determined by fits to the ΔE distribution in bins of $p\bar{p}$ invariant mass. The distribution from a three-body phase space MC normalized to the area of the signal is superimposed. It is clear that the observed mass distribution is not consistent with three-body phase space but instead is peaked at low $p\bar{p}$ mass. This feature is suggestive of quasi two-body decay.²⁰ It is also possible that the decay is a genuine three-body process and that this feature of the $M_{p\bar{p}}$ spectrum is a baryon form factor effect.^{21,22}

To avoid model dependence in the determination of the branching fraction for $p\bar{p}K^+$, we fit the ΔE signal yield in bins of $M(p\bar{p})$ and correct for the detection efficiency in each bin using a

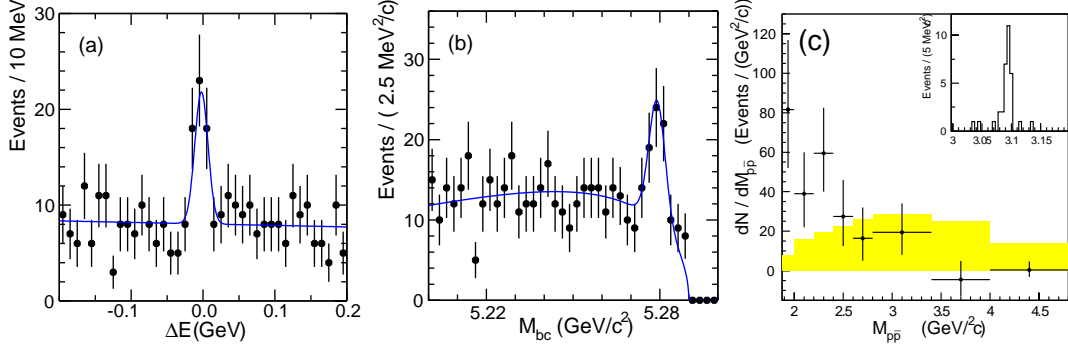


Figure 6: (a) ΔE and (b) M_{bc} distributions for $B^+ \rightarrow p\bar{p}K^+$ candidates. (c) The fitted yield divided by the bin size for $B^+ \rightarrow p\bar{p}K^+$ as a function of $M_{p\bar{p}}$. The distribution from non-resonant $B^+ \rightarrow p\bar{p}K^+$ MC simulation is superimposed. The inset shows the $M_{p\bar{p}}$ distribution for the $J/\psi K^+$ signal region by removing the charm veto.

three-body phase space $B^+ \rightarrow p\bar{p}K^+$ MC model. We then sum the partial branching fractions in each bin to obtain

$$\mathcal{B}(B^+ \rightarrow p\bar{p}K^+) = (4.3_{-0.9}^{+1.1}(\text{stat}) \pm 0.5(\text{syst})) \times 10^{-6}.$$

To verify the analysis procedure and branching fraction determination, we remove the J/ψ veto and examine the decay chain $B^+ \rightarrow J/\psi K^+$, $J/\psi \rightarrow p\bar{p}$. The $p\bar{p}$ invariant mass spectrum for $J/\psi K^+$ signal candidates is shown as an inset in Figure 6(c). The obtained branching fraction is in good agreement with the PDG world average.

For $B^0 \rightarrow p\bar{p}K_S^0$ and $B^+ \rightarrow p\bar{p}\pi^+$ modes, after the application of the charm and Λ_c vetoes, no significant signals are observed. A fit to the ΔE distributions to $p\bar{p}K_S^0$ gives $6.4_{-3.7}^{+4.4}$ events and $p\bar{p}\pi^\pm$ gives $16.2_{-8.0}^{+8.6}$ events with significance of 2.1σ . Applying the Feldman-Cousins procedure,²³ we obtain an upper limit at 90% C.L. of $\mathcal{B}(B^0 \rightarrow p\bar{p}K^0) < 7.2 \times 10^{-6}$ and $\mathcal{B}(B^+ \rightarrow p\bar{p}\pi^+) < 3.7 \times 10^{-6}$.

5 Search for Direct CP Violation

The most straightforward indication for CP violation in the B meson system would be a time-independent rate asymmetry between CP conjugate decays into flavor specific or self-tagging final states. Direct CP violation (DCPV) of this type will occur in a decay containing at least two amplitudes that have different CP conserving and CP violating phases. The charge asymmetry will be most evident in decays where the two amplitudes are of comparable strength. The partial rate asymmetry can be written as

$$\mathcal{A}_{CP} = \frac{N(\bar{B} \rightarrow \bar{f}) - N(B \rightarrow f)}{N(\bar{B} \rightarrow \bar{f}) + N(B \rightarrow f)} = \frac{2|A_1||A_2|\sin\delta\sin\phi}{|A_1|^2 + |A_2|^2 + 2|A_1||A_2|\cos\delta\cos\phi},$$

where δ and ϕ are the CP conserving and CP violating relative phases between amplitudes A_1 and A_2 ; B represents either a B_d^0 or B^+ meson, f represents a self tagging final state, and \bar{B} and \bar{f} are the conjugate states. In the Standard Model, DCPV occurs in charmless hadronic B decay modes that involve both penguin (P) amplitudes and weak $b \rightarrow u$ tree (T) amplitudes containing the CP violating weak phase $\phi_3 = \arg(V_{ub}^*)$ (in a standard convention²⁴).

We search for direct CP violation in the $B \rightarrow K^+\pi^-$, $K^+\pi^0$, $K_S^0\pi^+$, and ωK^+ decay modes by measuring the difference between the yields of \bar{B} and B decays into the self tagging final states. The asymmetries obtained are summarized in Table 3. All the results are consistent with null asymmetry, hence we set 90% C.L. limits. Note that the systematic bias from charge asymmetry in the detectors is less than 1%, much smaller than the statistical errors at present.

Table 3: Results of searches for direct CP violation.

mode	N(B)	N(\bar{B})	\mathcal{A}_{cp}	90% C.L.
$K^+\pi^-$	103 ± 12	115 ± 14	$-0.06 \pm 0.08 \pm 0.01$	-0.20:0.09
$K^+\pi^0$	28 ± 8	30 ± 8	$-0.04 \pm 0.19 \pm 0.03$	-0.39:0.30
$K_S^0\pi^+$	49 ± 8	18 ± 6	$0.46 \pm 0.15 \pm 0.02$	0.18:0.73
$\pi^+\pi^0$	24 ± 8	13 ± 7	$0.31 \pm 0.31 \pm 0.05$	-0.25:0.89
ωK^+	7.4 ± 3.5	11.6 ± 3.7	$-0.22 \pm 0.27 \pm 0.04$	-0.70 : 0.26

6 Summary

We have made the first observation of charmless baryonic decay $B^\pm \rightarrow p\bar{p}K^\pm$, the three-body $B^0 \rightarrow K^0\pi^+\pi^-$ and $B^0 \rightarrow K^0K^+K^-$, and see strong evidence of $B^\pm \rightarrow \eta K^\pm$ and $B^\pm \rightarrow \eta\pi^\pm$. We also observed the decay $B^\pm \rightarrow \omega K^\pm$ and measured the branching fractions for the decays $B \rightarrow K\pi$ and $\pi\pi$. We find no evidence for direct CP violation in the observed decays. By summer 2002 it is anticipated that Belle will have collected 90 fb^{-1} of data providing a rich sample to continue the search for rare B decays and measure CP violating effects in a variety of B decay modes.

References

1. Belle Collaboration, A. Abashian *et al.*, KEK Progress Report 2000-4 (2000), to appear in Nucl. Inst. and Meth. A.
2. KEKB B Factory Design Report, KEK Report 95-7 (1995), unpublished.
3. N. Cabibbo, Phys. Rev. Lett. **10**, 531 (1963); M. Kobayashi and T. Maskawa, Prog. Theor. Phys. **49**, 652 (1973).
4. A. J. Buras and R. Fleischer, Eur. Phys. J. C **16**, 96 (2000); M. Beneke, G. Buchlla, M. Neubert, and C. T. Sachrajda, Nucl. Phys. **B591**, 313 (2000); Y. Y. Keum, H. N. Li, and A. I. Sanda, Phys. Rev. D **63**, 054008 (2001).
5. CLEO Collaboration, S. J. Richichi *et al.*, Phys. Rev. Lett. **85**, 520 (2000).
6. BABAR Collaboration, B. Aubert *et al.*, Phys. Rev. Lett. **87**, 221802 (2001).
7. C.-W. Chiang and J. L. Rosner, hep-ph/0112285.
8. Particle Data Group, D. E. Groom *et al.*, Eur. Phys. J. C **15**, 1 (2000).
9. J. E. Gaiser *et al.*, Phys. Rev. D **34**, 711 (1986).
10. H. Albrecht *et al.*, Phys. Lett. **B241**, 278 (1990).
11. CLEO Collaboration, C.P. Jessop *et al.*, Phys. Rev. Lett. **85**, 2881 (2000).
12. Belle Collaboration, A. Garmash *et al.*, Phys. Rev. D **65**, 092005 (2002).
13. CLEO Collaboration, X. Fu *et al.*, Phys. Rev. Lett. **79**, 3125 (1997).
14. CLEO Collaboration, T.E. Coan *et al.*, Phys. Rev. D **59**, 111101 (1999); CLEO Collaboration, T. Bergfeld *et al.*, Phys. Rev. Lett. **77**, 4503 (1996).
15. ARGUS Collaboration, H. Albrecht *et al.*, Phys. Lett. B **209**, 119 (1988).
16. DELPHI Collaboration, P. Abreu *et al.* Phys. Lett. B **357**, 255 (1995); DELPHI Collaboration, W. Adam *et al.* Z. Phys. C **72**, 207 (1996).
17. Belle Collaboration, K. Abe *et al.*, Phys. Rev. D **65**, 091103(R) (2002).
18. Belle Collaboration, K. Abe *et al.*, Phys. Rev. Lett. **88**, 181803 (2002).
19. G. Eilam, M. Gronau, and J. Rosner, Phys. Rev. D **39**, 819 (1989).
20. C.-K. Chua, W.-S. Hou, and S.-Y. Tsai, hep-ph/0204186.
21. C.-K. Chua, W.-S. Hou, and S.-Y. Tsai, hep-ph/0204185; Phys. Lett. **B528**, 233 (2002).
22. H.-Y. Cheng and K.-C. Yang, hep-ph/0112245.
23. G. J. Feldman and R. D. Cousins, Phys. Rev. D **57**, 3873 (1998).
24. L. Wolfenstein, Phys. Rev. Lett. **51**, 1945 (1983).